Article

Reactivity of the Indole Ring in Palladium(II) Complexes of 2N1O-Donor Ligands: Cyclopalladation and □-Cation Radical Formation

Takeshi Motoyama, Yuichi Shimazaki, Tatsuo Yajima, Yasuo Nakabayashi, Yoshinori Naruta, and Osamu Yamauchi

J. Am. Chem. Soc., **2004**, 126 (23), 7378-7385• DOI: 10.1021/ja031587v • Publication Date (Web): 18 May 2004

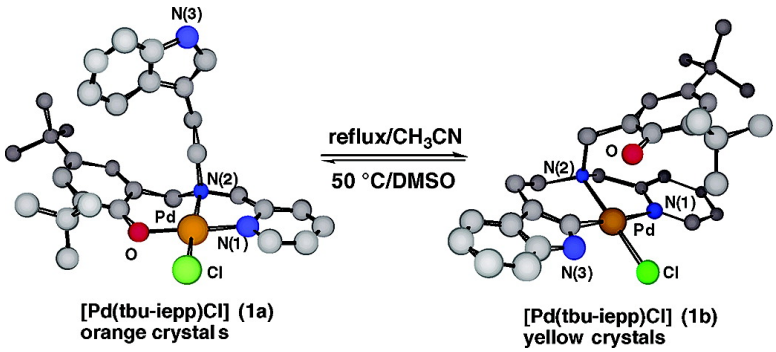

[Pd(tbu-iepp)Cl] (1a)
orange crystals

[Pd(tbu-iepp)Cl] (1b)
yellow crystals

More About This Article

Additional resources and features associated with this article are available within the HTML version:

- Supporting Information
- Access to high resolution figures
- Links to articles and content related to this article
- Copyright permission to reproduce figures and/or text from this article

View the Full Text HTML

J|A|C|S
ARTICLES
Published on Web 05/18/2004

Reactivity of the Indole Ring in Palladium(II) Complexes of 2N1O-Donor Ligands: Cyclopalladation and π-Cation Radical Formation

Takeshi Motoyama,[†] Yuichi Shimazaki,*[,‡] Tatsuo Yajima,[†] Yasuo Nakabayashi,[†] Yoshinori Naruta,[‡] and Osamu Yamauchi*[,†]

Contribution from the Unit of Chemistry, Faculty of Engineering, Kansai University, Suita, Osaka 564-8680, Japan, and Institute for Materials Chemistry and Engineering, Kyushu University, Higashi-ku, Fukuoka 812-8581, Japan

Received December 9, 2003; E-mail: yshima@ms.ifoc.kyushu-u.ac.jp; osamuy@ipcku.kansai-u.ac.jp

Abstract: The Pd(II) complexes of new 2N1O-donor ligands containing a pendent indole, 3-[*N*-2-pyridylmethyl-*N*-2-hydroxy-3,5-di(*tert*-butyl)benzylamino]ethylindole (Htbu-iepp), 1-methyl-3-[*N*-2-pyridylmethyl-*N*-2-hydroxy-3,5-di(*tert*-butyl)benzylamino]ethylindole (Htbu-miepp), 3-[*N*-2-pyridylmethyl-*N*-2-hydroxy-3,5-di(*tert*-butyl)benzylamino]methylindole (Htbu-impp), and 3-(*N*-2-pyridylmethyl-*N*-4-hydroxybenzylamino)ethylindole (Hp-iepp) (H denotes a dissociable proton), were synthesized, and the structures of [Pd(tbu-iepp)Cl] (**1a**), [Pd(tbu-iepp-c)Cl] (**1b**), [Pd(tbu-miepp)Cl] (**3**), and [Pd(p-iepp-c)Cl] (**4**) (tbu-iepp-c and p-iepp-c denote tbu-iepp and p-iepp bound to Pd(II) through a carbon atom, respectively) were determined by X-ray analysis. Complexes **1a** prepared in CH_2Cl_2/CH_3CN and **3** prepared in CH_3CN have a pyridine nitrogen, an amine nitrogen, a phenolate oxygen, and a chloride ion in the coordination plane. Complex **1b** prepared in CH_3CN has the same composition as **1a** and was revealed to have the C2 atom of the indole ring bound to Pd(II) with the Pd(II)−C2 distance of 1.973(2) Å. The same Pd(II)−indole C2 bonding was revealed for **4**. Interconversion between **1a** and **1b** was observed for their solutions, the equilibrium being dependent on the solvent used. Reaction of **1b** and **4** with 1 equiv of Ce(IV) in DMF gave the corresponding one-electron-oxidized species, which exhibited an ESR signal at $g = 2.004$ and an absorption peak at ∼550 nm, indicating the formation of the Pd(II)−indole π-cation radical species. The half-life, $t_{1/2}$, of the indole radical species at room temperature was calculated to be 20 s ($k_{obs} = 3.5 \times 10^{-2}$ s^{-1}) for **1b**. The cyclic voltammogram for **1b** in DMF gave two irreversible oxidation peaks at $E_{pa} = 0.68$ and 0.80 V (vs Ag/AgCl), which were ascribed to the oxidation processes of the coordinated indole and phenolate moieties, respectively.

Introduction

Aromatic amino acid residues play vital roles in the stabilization and functions of proteins.[1−3] The tyrosyl residue serves as an important metal binding site and forms the metal−phenoxyl radical species as has been established for Cu-containing galactose oxidase.[4,5] On the other hand, the indole ring of the tryptophyl residue with the highest hydrophobicity among α-amino acids[6] is known to form a hydrophobic environment for specific binding of molecules and to be involved in electron-transfer pathways.[7,8] Tryptophan (Trp) coordinates to metal ions through the amino and carboxylate groups and may undergo intramolecular stacking interactions[9−11] as typically revealed for [Cu(L)(Trp)]ClO_4 (L = 2,2′-bipyridine[12] or 1,10-phenanthroline[13]). The indole ring is not known to be involved in metal binding in biological systems, but it can form various metal−indole bonds in chemical systems. We reported earlier that alkylindoles coordinate to Pd(II) through the imine nitrogen atom of the tautomeric 3*H*-indole ring where the NH hydrogen atom is bound at the C3 atom.[14] Pd(II)−C3 bond formation was observed for the complex of indole-3-acetate (IA) in the 3*H*-indole form, [$Pd_2(IA)_2(py)_2$] (py = pyridine), where Pd(II) binds with IA to form a *spiro* ring through the carboxylate oxygen

[†] Kansai University.
[‡] Kyushu University.

(1) (a) Burley, S. K.; Petsko, G. A. *Science* **1985**, *229*, 23−28. (b) Burley, S. K.; Petsko, G. A. *Adv. Protein Chem.* **1988**, *39*, 125−189. (c) Burley, S. K.; Petsko, G. A. *J. Am. Chem. Soc.* **1986**, *108*, 7995−8001. (d) Serrano, L.; Bycroft, M.; Fersht, A. R. *J. Mol. Biol.* **1991**, *218*, 465−475. (e) Hunter, C. A.; Singh, J.; Thornton, J. M. *J. Mol. Biol.* **1991**, *218*, 837−846.
(2) Branden, C.; Tooze, J. *Introduction to Protein Structure*, 2nd ed.; Garland Publishing: New York, 1998.
(3) Meyer, E. A.; Castellano, R. K.; Diederich, F. *Angew. Chem., Int. Ed.* **2003**, *42*, 1210−1250.
(4) Stubbe, J.; van der Donk, W. A. *Chem. Rev.* **1998**, *98*, 705−762.
(5) Whittaker, J. W. *Met. Ions Biol. Syst.* **1994**, *30*, 315−360.
(6) Nozaki, Y.; Tanford, C. *J. Biol. Chem.* **1971**, *246*, 2211−2217.
(7) Isied, S. S. *Met. Ions Biol. Syst.* **1991**, *27*, 1−56.
(8) Nocek, J. M.; Zhou, J. S.; de Frost, S.; Priyadarshy, S.; Beratan, D. N.; Onuchic, J. N.; Hoffman, B. M. *Chem. Rev.* **1996**, *96*, 2459−2489.
(9) (a) Fischer, B. E.; Sigel, H. *J. Am. Chem. Soc.* **1980**, *102*, 2998−3008. (b) Guogang, L.; Sigel, H. *Z. Naturforsch.* **1989**, *44b*, 1555−1566.
(10) Yamauchi, O.; Odani, A.; Hirota, S. *Bull. Chem. Soc. Jpn.* **2001**, *74*, 1525−1545.
(11) Yamauchi, O.; Odani, A.; Takani, M. *J. Chem. Soc., Dalton Trans.* **2002**, 3411−3421 and references therein.
(12) Masuda, H.; Sugimori, T.; Odani, A.; Yamauchi, O. *Inorg. Chim. Acta* **1991**, *180*, 73−79.
(13) Aoki, K.; Yamazaki, H. *J. Chem. Soc., Dalton Trans.* **1987**, 2017−2021.
(14) Yamauchi, O.; Takani, M.; Toyoda, K.; Masuda, H. *Inorg. Chem.* **1990**, *29*, 1856−1860.

10.1021/ja031587v CCC: $27.50

and C3 atoms with deprotonation.[15] Kostić et al. developed unique artificial peptidases using Pd(II) and Pt(II) which recognize the indole moiety and cleave the adjacent amide or peptide bond specifically.[16] Other examples are also known for Pd(II)−indole C2 bonding as a result of a cyclopalladation-like reaction.[17] The pendent indole ring in metal complexes of tripodal ligands, where one of the coordinating groups was replaced with an indole ring, was found to bind with Cu(I) by η^2-type coordination of the C2═C3 bond to form a tetrahedral structure.[18]

On the other hand, formation of the indolyl radical from a tryptophyl residue in proteins has been established for the intermediate, compound I, formed in the catalytic reaction of cytochrome *c* peroxidase (CcP).[4,7,8,19,20] Indolyl radical formation is possible with other biological systems,[4] and more recently Gray et al. reported the formation of the photogenerated tryptophan radical in modified azurins.[21] Indole radicals in chemical systems have been generated by pulse radiolysis,[22] but their characterization has been difficult because of the instability. We observed previously that the Cu(I) complex of the *N*,*N*-bis(3-indolyl)methyl derivative of 2-aminomethylpyridine in CH_2Cl_2 reacted with dioxygen to form a $Cu^{III}_2(\mu\text{-}O)_2$ intermediate, giving a compound with a bis(indolyl) moiety with a *spiro* ring structure as a decomposition product.[23] This strongly suggested that the bis(indolyl) structure resulted from the coupling of two vicinal indolyl radicals, although we could not detect radical species in the course of the reaction.

With these points in mind, we now investigated the behavior of the pendent indole ring in the Pd(II) complexes of 2N1O-donor ligands involving a phenol, a pyridine, and a tertiary amine as metal binding sites (Figure 1). The indole ring exhibited a stacking interaction with the coordinated pyridine ring and replaced the phenolate group under suitable conditions to form complexes with a direct Pd(II)−C2 bond, which were shown to give the indole π-cation radical species upon oxidation with cerium(IV).

Experimental Section

Materials. Indole and sodium cyanoborohydride were obtained from Tokyo Kasei, triethylamine was from Wako, and $PdCl_2$ was from Aldrich. All of the chemicals used were of the highest grade available and were further purified whenever necessary.[24] Solvents were also purified before use by standard methods.[24] DMSO-d_6 was purchased from the Cambridge Isotope Laboratory.

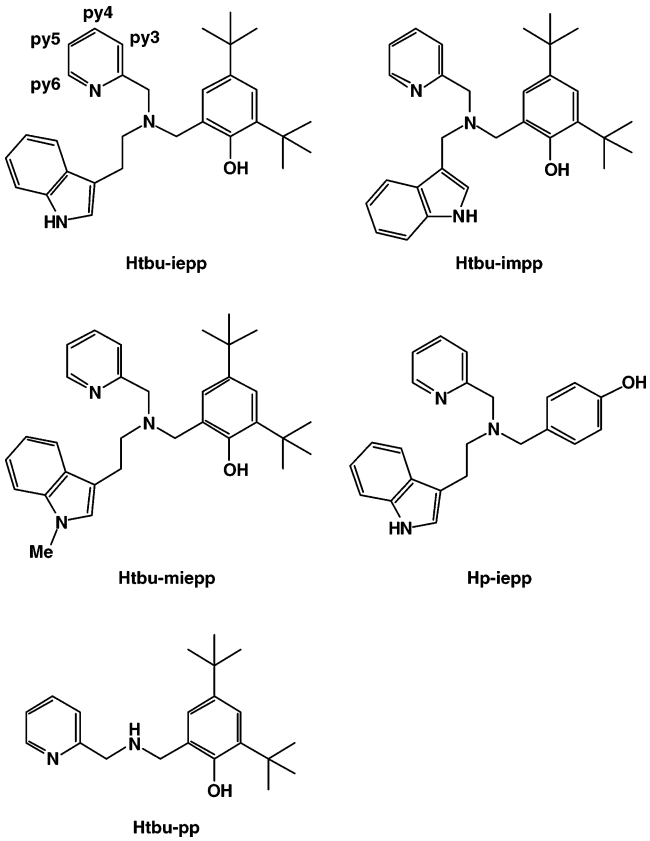

Figure 1. Structures of ligands.

3-[*N*-2-Pyridylmethyl-*N*-2-hydroxy-3,5-di(*tert*-butyl)benzylamino]-ethylindole (Htbu-iepp). To a solution of 3,5-di(*tert*-butyl)salicylaldehyde[25] (2.34 g, 10 mmol) and 3-(*N*-2-pyridylmethylamino)ethylindole[23,26] (2.6 g, 10 mmol) in methanol (50 mL) was carefully added sodium cyanoborohydride (0.63 g, 10 mmol). The resulting solution was stirred for 6 h to give a white powder, which was recrystallized from $CH_3COOC_2H_5$. Yield: 2.14 g (45%). ^{1}H NMR (400 MHz, $CDCl_3$): δ (vs TMS) 10.83 (br, 1H), 8.52 (d, 1H), 7.92 (s, 1H), 7.54 (t, 1H), 7.20 (m, 4H), 7.11 (m, 2H), 7.00 (t, 1H), 6.98 (s, 1H), 6.95 (s, 1H), 3.93 (s, 2H), 3.89 (s, 2H), 2.97 (m, 4H), 1.44 (s, 9H), 1.28 (s, 9H).

3-[*N*-2-Pyridylmethyl-*N*-2-hydroxy-3,5-di(*tert*-butyl)benzylamino]-methylindole (Htbu-impp). Indole (0.73 g, 6.2 mmol) and *N*-2-pyridylmethyl-*N*-2-hydroxy-3,5-di(*tert*-butyl)benzylamine[25] (2.03 g, 6.22 mmol) were dissolved in methanol (50 mL), to which an aqueous solution of formaldehyde (0.50 g, 6.2 mmol) and a small amount of acetic acid were added. The resulting solution was stirred for 6 h to give a white powder, which was recrystallized from $CH_3COOC_2H_5$. Yield: 2.0 g (72%). ^{1}H NMR (400 MHz, $CDCl_3$): δ (vs TMS) 11.04 (br, 1H), 8.56 (d, 1H), 8.16 (s, 1H), 7.65 (m, 2H), 7.36 (d, 2H), 7.27 (d, 2H), 7.14 (m, 3H), 6.85 (d, 1H), 3.93 (s, 2H), 3.84 (s, 2H), 3.83 (s, 2H), 1.46 (s, 9H), 1.26 (s, 9H).

1-Methyl-3-[*N*-2-Pyridylmethyl-*N*-2-hydroxy-3,5-di(*tert*-butyl)-benzylamino]ethylindole (Htbu-miepp). Htbu-miepp was prepared in a manner similar to that described for Htbu-iepp from 3,5-di(*tert*-butyl)-salicylaldehyde[25] (2.3 g, 10 mmol) and 1-methyl-3-(*N*-2-pyridylmethylamino)ethylindole (2.7 g, 10 mmol).[26,27] Yield: 3.6 g (75%). ^{1}H NMR (400 MHz, $CDCl_3$): δ (vs TMS) 8.46 (d, 1H), 7.65 (s, 1H), 7.52 (t,

(15) Takani, M.; Masuda, H.; Yamauchi, O. *Inorg. Chim. Acta* **1995**, *235*, 367−374.
(16) (a) Kaminskaia, N. V.; Johnson, T. W.; Kostić, N. M. *J. Am. Chem. Soc.* **1999**, *121*, 8663−8664. (b) Kaminskaia, N. V.; Ullmann, G. M.; Fulton, D. B.; Kostić, N. M. *Inorg. Chem.* **2000**, *39*, 5004−5013. (c) Kaminskaia, N. V.; Kostić, N. M. *Inorg. Chem.* **2001**, *40*, 2368−2377. (d) Milović, N. M.; Kostić, N. M. *Met. Ions Biol. Syst.* **2001**, *38*, 145−186.
(17) Robson, R. *Inorg. Chim. Acta* **1982**, *57*, 71−77.
(18) Shimazaki, Y.; Yokoyama, H.; Yamauchi, O. *Angew. Chem., Int. Ed.* **1999**, *38*, 2401−2403.
(19) Sivaraja, M.; Goodin, D. B.; Smith, M.; Hoffman, B. M. *Science* **1989**, *245*, 738−740.
(20) Poulos, T. L.; Fenna, R. E. *Met. Ions Biol. Syst.* **1994**, *30*, 25−75.
(21) Di Bilio, A. J.; Crane, B. R.; Wehbi, W. A.; Kiser, C. N.; Abu-Omar, M. M.; Carlos, R. M.; Richards, J. H.; Winkler, J. R.; Gray, H. B. *J. Am. Chem. Soc.* **2001**, *123*, 3181−3182.
(22) (a) DeFelippis, M. R.; Murthy, C. P.; Broitman, F.; Weinraub, D.; Faraggi, M.; Klapper, M. H. *J. Phys. Chem.* **1991**, *95*, 3416−3419. (b) Solar, S.; Getoff, N.; Surdhar, P. S.; Armstrong, D. A.; Singh, A. *J. Phys. Chem.* **1991**, *95*, 3639−3643.
(23) Shimazaki, Y.; Nogami, T.; Tani, F.; Odani, A.; Yamauchi, O. *Angew. Chem., Int. Ed.* **2001**, *40*, 3859−3862.
(24) Perrin, D. D.; Armarego, W. L. F.; Perrin, D. R. *Purification of Laboratory Chemicals*; Pergamon Press: Elmsford, NY, 1966.
(25) (a) Shimazaki, Y.; Huth, S.; Hirota, S.; Yamauchi, O. *Bull. Chem. Soc. Jpn.* **2000**, *73*, 1187−1195. (b) Shimazaki, Y.; Huth, S.; Odani, A.; Yamauchi, O. *Angew. Chem., Int. Ed.* **2000**, *39*, 1666−1669.
(26) Yajima, T.; Shimazaki, Y.; Ishigami, N.; Odani, A.; Yamauchi, O. *Inorg. Chim. Acta* **2002**, *337*, 193−202.
(27) Kuehne, M. E.; Huebner, J. A.; Matsko, T. H. *J. Org. Chem.* **1979**, *44*, 2477−2480.

1H), 7.25 (m, 2H), 7.15 (t, 1H), 7.11 (q, 1H), 6.96 (t, 1H), 6.87 (t, 2H), 6.79 (s, 1H), 3.91 (s, 2H), 3.85 (s, 2H), 3.69 (s, 3H), 2.95 (m, 4H), 1.43 (s, 9H), 1.41 (s, 9H).

3-(*N*-2-Pyridylmethyl-*N*-4-hydroxybenzylamino)ethylindole (Hp-iepp). Hp-iepp was prepared in a manner similar to that described for Htbu-iepp from 4-hydroxybenzaldehyde (1.2 g, 10 mmol) and 3-(*N*-2-pyridylmethylamino)ethylindole (2.6 g, 10 mmol). Yield: 2.02 g (57%). ^{1}H NMR (400 MHz, DMSO-d_6): δ (vs TMS) 10.72 (br, 1H), 9.29 (s, 1H), 8.45 (d, 1H), 7.70 (t, 2H), 7.46 (d, 2H), 7.20 (m, 2H), 7.01 (t, 2H), 6.87 (t, 2H), 6.70 (d, 2H), 3.16 (s, 2H), 2.70 (t, 2H), 2.67 (t, 2H), 2.50 (s, 2H).

***N*-2-Pyridylmethyl-*N*-2-hydroxy-3,5-di(*tert*-butyl)benzylamine (Htbu-pep).** To a solution of 2-pyridylmethylamine (1.08 g, 10 mmol) in methanol (100 mL) was added 3,5-di(*tert*-butyl)salicylaldehyde (2.34 g, 10 mmol), and to the resulting solution was carefully added sodium tetrahydroborate (0.30 g, 8 mmol) with stirring. The reaction mixture was then stirred for 12 h at room temperature, acidified by addition of concentrated HCl, and evaporated almost to dryness under a reduced pressure. The residue was dissolved in saturated aqueous Na_2CO_3 (50 mL) and extracted with three 100-mL portions of $CHCl_3$. The combined extracts were dried over Na_2SO_4 and evaporated almost to dryness under a reduced pressure to give a white powder, which was recrystallized from diethyl ether. Yield: 2.22 g (68%). ^{1}H NMR (400 MHz, DMSO-d_6): δ (vs TMS) 8.53 (d, 1H), 7.78 (t, 1H), 7.37 (d, 1H), 7.28 (t, 1H), 7.08 (d, 1H), 6.85 (d, 1H), 3.87 (s, 2H), 3.84 (s, 2H), 1.35 (s, 9H), 1.22 (s, 9H).

[Pd(tbu-iepp)Cl] (1a). To a solution of Htbu-iepp (0.47 g, 1.0 mmol) in 1:1 (v/v) CH_2Cl_2/CH_3CN (20 mL) was added $PdCl_2$ (0.18 g, 1.0 mmol). A few drops of triethylamine were added to the resulting solution, which was stirred overnight at room temperature to give orange crystals. Anal. Calcd for **1a** ($C_{31}H_{38}N_3OClPd$): C, 60.99; H, 6.27; N, 6.88. Found: C, 60.88; H, 6.31; N, 6.89. ^{1}H NMR (400 MHz, DMSO-d_6): δ (vs TMS) 10.74 (s, 1H), 8.69 (d, 1H), 8.11 (t, 1H), 7.77 (d, 1H), 7.52 (t, 1H), 7.23 (d, 1H), 7.10 (s, 1H), 7.09 (s, 1H), 6.96 (t, 1H), 6.88 (d, 1H), 6.71 (m, 2H), 5.47 (d, 1H), 4.64 (d, 1H), 4.48 (d, 1H), 3.75 (d, 1H), 2.99 (m, 2H), 2.85 (m, 1H), 2.70 (m, 1H), 1.36 (s, 9H), 1.22 (s, 9H).

[Pd(tbu-iepp-c)Cl] (1b). To a suspension of Htbu-iepp (0.47 g, 1.0 mmol) in CH_3CN (20 mL) was added $PdCl_2$ (0.18 g, 1.0 mmol). A few drops of triethylamine were added to the resulting solution, which was refluxed overnight to give yellow crystals. Anal. Calcd for **1b** ($C_{31}H_{38}N_3OClPd$): C, 60.99; H, 6.27; N, 6.88. Found: C, 60.85; H, 6.41; N, 6.89. ^{1}H NMR (400 MHz, DMSO-d_6): δ (vs TMS) 9.52 (s, 1H), 8.44 (d, 1H), 8.34 (s, 1H), 8.09 (d, 1H), 7.65 (t, 1H), 7.36 (q, 1H), 7.29 (q, 1H), 7.15 (m, 2H), 6.84 (m, 3H), 4.74 (d, 1H), 4.43 (d, 1H), 4.07 (q, 2H), 3.77 (m, 1H), 3.41 (m, 1H), 1.23 (s, 9H), 1.20 (s, 9H).

[Pd(tbu-impp)Cl] (2), [Pd(tbu-miepp)Cl] (3), [Pd(p-iepp-c)Cl]·CH_3CN (4), and [Pd(tbu-pp)Cl] (5). These complexes were prepared in a manner similar to that described for **1b** as orange crystals (**2**, **3**, and **5**) and yellow crystals (**4**), respectively. Anal. Calcd for **2** ($C_{30}H_{36}N_3OClPd$): C, 60.41; H, 6.08; N, 7.04. Found: C, 60.38; H, 6.08; N, 7.05. ^{1}H NMR (400 MHz, DMSO-d_6): δ (vs TMS) 10.97 (br, 1H), 8.22 (d, 1H), 8.04 (d, 1H), 7.59 (t, 1H), 7.28 (d, 1H), 7.10 (m, 3H), 7.01 (m, 3H), 6.91 (t, 1H), 4.94 (d, 1H), 4.80 (d, 1H), 4.17 (d, 1H), 4.00 (d, 1H), 3.60 (d, 1H), 3.47 (d, 1H), 1.44 (s, 9H), 1.26 (s, 9H). Anal. Calcd for **3** ($C_{32}H_{40}N_3OClPd$): C, 61.54; H, 6.46; N, 6.73. Found: C, 61.48; H, 6.48; N, 6.75. ^{1}H NMR (400 MHz, DMSO-d_6): δ (vs TMS) 8.65 (d, 1H), 8.07 (t, 1H), 7.76 (d, 1H), 7.47 (t, 1H), 7.22 (d, 1H), 7.11 (d, 1H), 7.04 (d, 1H), 7.00 (t, 1H), 6.86 (s, 1H), 6.72 (t, 1H), 6.66 (d, 1H), 5.00 (d, 1H), 4.65 (d, 1H), 4.48 (d, 1H), 3.72 (d, 1H), 3.61 (s, 3H), 3.37 (d, 1H), 2.97 (m, 3H), 2.67 (m, 1H), 1.37 (s, 9H), 1.23 (s, 9H). Anal. Calcd for **4** ($C_{24}H_{23}N_3OClPd·CH_3CN$): C, 55.57; H, 4.85; N, 10.37. Found: C, 55.54; H, 4.83; N, 10.44. ^{1}H NMR (400 MHz, DMSO-d_6): δ (vs TMS) 9.45 (br, 1H), 9.45 (br, 1H), 8.53 (d, 1H), 7.83 (t, 1H), 7.30 (m, 6H), 6.84 (m, 2H), 6.47 (d, 2H), 4.75 (d, 1H), 4.31 (d, 1H), 4.20 (d, 1H), 3.68 (d, 1H), 3.59 (td, 2H), 3.22 (d, 1H), 3.14 (d, 1H). Anal. Calcd for **5** ($C_{21}H_{29}N_2OClPd$): C, 53.97; H, 6.25; N, 5.99. Found: C, 53.54; H, 6.23; N, 5.84. ^{1}H NMR (400 MHz, DMSO-d_6): δ (vs TMS) 8.67 (d, 1H), 8.02 (t, 1H), 7.63 (d, 1H), 7.48 (t, 1H), 7.01 (d, 2H), 6.96 (br, 1H), 6.89 (d, 1H), 4.66 (q, 1H), 4.06 (m, 2H), 3.45 (t, 1H), 1.35 (s, 9H), 1.21 (s, 9H).

X-ray Structure Determination. The X-ray experiments were carried out for the well-shaped single crystal of complex **1b** on a Rigaku RAXIS imaging plate area detector with graphite monochromated Mo Kα radiation (λ = 0.71073 Å). The crystal was mounted on a glass fiber. To determine the cell constants and orientation matrix, three oscillation photographs were taken for each frame with an oscillation angle of 3° and an exposure time of 3 min. The X-ray experiments for **1a**, **3**, and **4** were carried out on a Rigaku MSC Mercury CCD diffractometer with graphite monochromated Mo Kα radiation (λ = 0.71073 Å). For the determination of the cell constants and orientation matrix, six oscillation photographs were taken for each frame with an oscillation angle of 0.3° and an exposure time of 10 s. Intensity data were collected by taking oscillation photographs. Refraction data were corrected for both Lorentz and polarization effects. The structures were solved by the direct method and refined anisotropically for non-hydrogen atoms by full-matrix least-squares calculations except for the disordered terminal carbons of one of the *tert*-butyl groups in complex **3**. The treatment of the disordered carbons in **3** was made in such a way that the six apparent carbons were placed on the *tert*-butyl group, and the occupancy of each carbon was obtained by calculation. All of the disordered carbons were refined isotropically. Each refinement was continued until all shifts were smaller than one-third of the standard deviations of the parameters involved. Atomic scattering factors were taken from the literature.[28] Except for the hydrogen atoms of the phenol OH group and the disordered carbons in **3**, all hydrogen atoms were located at the calculated positions, assigned a fixed displacement, and constrained to ideal geometry with C−H = 0.95 Å and N−H = 0.90 Å. The thermal parameters of calculated hydrogen atoms were related to those of their parent atoms by $U(H) = 1.2U_{eq}(C,N)$. The hydrogen atoms of the phenol OH groups were located from the difference Fourier maps, while no hydrogen atoms were assigned to the disordered carbons in **3**. All of the calculations were performed by using the TEXSAN crystallographic software program package from the Molecular Structure Corp.[29] Summaries of the fundamental crystal data and experimental parameters for the structure determination of complexes **1a**, **1b**, **3**, and **4** are given in Table 1.

Spectroscopies. Electronic spectra were measured with a Shimadzu UV-3101PC spectrophotometer. NMR measurements were performed with a JEOL JNM-GSX-400 (400 MHz) NMR spectrometer. Frozen solution ESR spectra were taken at 77 K in quartz tubes with a 4-mm inner diameter on a JEOL JES-RE1X X-band spectrometer equipped with a standard low-temperature apparatus. The *g* values were calibrated with a Mn(II) marker used as a reference.

Collection of NMR Data for the van't Hoff Plot. The ^{1}H NMR data were measured for each of five 1-mL aliquots of 1 mM **1b** in DMSO-d_6 after keeping them in a bath thermostated at 20, 30, 40, 50, and 60 °C, respectively. The average values of concentrations of **1a**, which were calculated from the data collected from five independent measurements, were used for the van't Hoff plot.

Electrochemistry. Redox potentials of **1a** and **1b** (1.0 mM) in dried DMF containing 0.1 M tetra-*n*-butylammonium perchlorate (TBAP) as supporting electrolyte were determined at room temperature under deaerated conditions by cyclic voltammetry using a BAS 100B electrochemical analyzer with a three-electrode system. A glassy-carbon and a platinum wire were used as the working electrode and the counter electrode, respectively. The reversibility of the electrochemical processes

(28) Ibers, J. A.; Hamilton, W. C. *International Tables for X-ray Crystallography*; Kynoch: Birmingham, 1974; Vol. IV.
(29) Crystal Structure Analysis Package, Molecular Structure Corp., 1985 and 1999.

Table 1. Crystallographic Data

	1a	1b	3	4
formula	$PdC_{31}H_{38}N_3OCl$	$PdC_{31}H_{38}N_3OCl$	$PdC_{32}H_{40}N_3OCl$	$Pd_2C_{52}H_{53}N_9O_2Cl_2$
formula weight	610.51	610.51	624.54	1119.76
crystal color, habit	orange, platelet	yellow, prism	orange, needle	yellow, prism
crystal dimensions (mm)	0.45 × 0.16 × 0.02	0.12 × 0.23 × 0.21	0.18 × 0.03 × 0.05	0.26 × 0.12 × 0.10
crystal system	orthorhombic	monoclinic	monoclinic	monoclinic
a (Å)	17.276(5)	8.5354(6)	11.777(2)	12.252(2)
b (Å)	69.1(1)	15.3198(9)	8.450(2)	14.313(2)
c (Å)	9.519(2)	21.615(2)	30.106(6)	15.292(2)
α (deg)				76.069(9)
β (deg)		87.961(3)	96.9551(9)	69.391(8)
γ (deg)				86.72(1)
V (Å^3)	11 364(17)	2824.6(4)	2974(1)	2435.0(6)
space group	*Fdd*2	$P2_1/n$	$P2_1/n$	*P*-1
Z value	16	4	4	2
D_{calc} (g/cm^3)	1.427	1.436	1.395	1.527
F(000)	5056.00	1264.00	1296.00	1140.00
μ (Mo Kα)/cm^{-1}	7.76	7.81	7.43	9.00
$2\theta_{max}$/deg	55.0	55.0	55.0	55.0
observed reflns	21 911	26 676	23 270	21 652
independent reflns	6015	6438	6566	10 870
reflns used	6015	6438	6566	10 870
no. of variables	335	334	343	604
R_1 [$I > 2\sigma(I)$][a]	0.038	0.030	0.040	0.047
R_w (all data)[b]	0.101	0.077	0.108	0.114

[a] $R_1 = \sum||F_o| - |F_c||/\sum|F_o|$ for $I > 2\sigma(I)$ data. [b] $R_w = \{\sum\omega(|F_o| - |F_c|)^2/\sum\omega F_o^2\}^{1/2}$; $\omega = 1/\sigma^2(F_o) = \{\sigma_c^2(F_o) + p^2/4 \cdot F_o^2\}^{-1}$.

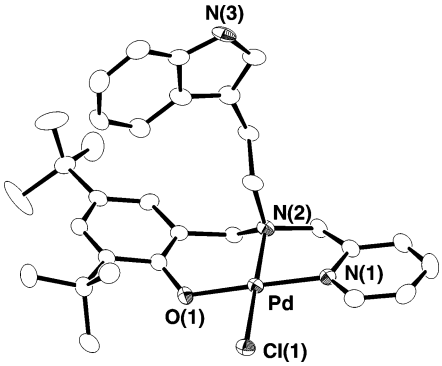

Figure 2. ORTEP view of [Pd(tbu-iepp)Cl] (**1a**) drawn with the thermal ellipsoids at the 50% probability level and the atomic labeling scheme.

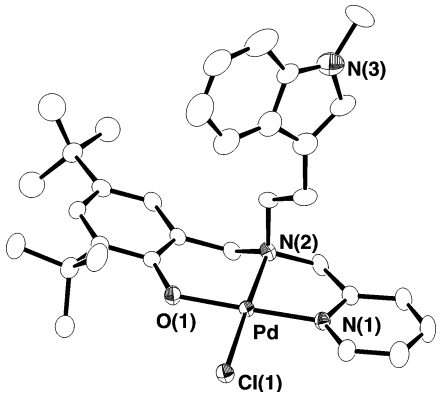

Figure 3. ORTEP view of [Pd(tbu-miepp)Cl] (**3**) drawn with the thermal ellipsoids at the 50% probability level and the atomic labeling scheme.

was evaluated by standard procedures, and all potentials were recorded against the Ag/AgCl reference electrode which was calibrated with the ferrocene/ferrocenium redox couple.

Results and Discussion

Preparation and Structures of Pd(II) Complexes. 2N1O-donor tripod-like ligands, Htbu-iepp and Htbu-impp where H denotes a dissociable proton, reacted with $PdCl_2$ and triethylamine in 1:1 (v/v) CH_2Cl_2/C_2H_5OH at room temperature to give [Pd(tbu-iepp)Cl] (**1a**) and [Pd(tbu-impp)Cl] (**2**), respectively, as orange crystals. A complex containing an *N*-methyltryptamine moiety, [Pd(tbu-miepp)Cl] (**3**), was also obtained as an orange powder by the reaction in CH_3CN at 80 °C. X-ray crystal structure analysis revealed that **1a** and **3** have a mononuclear square-planar geometry formed by a phenolate oxygen, an amine nitrogen, a pyridine nitrogen, and a chloride ion, as shown in Figures 2 and 3, respectively. Complex **2** having a ligand very similar to that of **1a** and **3** is inferred to have the same coordination structure. The Pd−N and Pd−O bond lengths of these complexes (Pd−N = 2.00−2.08; Pd−O = 1.97−2.00 Å) (Table 2) correspond well with those reported for Pd(II) complexes.[26,30] The side-chain indole ring of **1a** and **3** is not coordinated and is without any interactions within the complex molecule.

The reactions of Htbu-iepp and Hp-iepp with $PdCl_2$ in CH_3CN with refluxing gave [Pd(tbu-iepp-c)Cl] (**1b**) and [Pd(p-iepp-c)Cl]·CH_3CN (**4**), respectively, as yellow crystals. Complex **1b** was also obtained by refluxing **1a** in CH_3CN for 12 h and was found to have the same formula as **1a**. No such conversion was observed for **2**, where a methylene group instead of an ethylene group bridges the tertiary nitrogen atom and the indole ring. Complexes **1b** and **4** were disclosed to have the structures shown in Figures 4 and 5, respectively, where the Pd(II) ion binds with the C2 atom of the indole ring in addition to the amine and pyridine nitrogens in a square-planar geometry. The unit cell of **4** consists of two crystallographically independent Pd(II) complexes and three CH_3CN molecules. The Pd−N, Pd−C, and Pd−Cl bond lengths of **1b** and **4** (Pd−N = 2.07−2.11; Pd(1)−C = 1.97−1.98; Pd−Cl = 2.31−2.32 Å) (Table 2) are within the ranges reported for Pd(II) complexes.[26,31] As compared with **1a**, **1b** and **4** have a longer Pd−N(1) distance,

(30) Barnard, C. T. J.; Russel, M. J. H. In *Comprehensive Coordination Chemistry*; Wilkinson, G., Gillard, R. D., McCleverty, J. A., Eds.; Pergamon: Oxford, 1987; Vol. 5, Chapter 53.

Table 2. Selected Bond Lengths (Å) and Angles (deg) for **1**, **3**, and **4**

				4	
	1a	**1b**	**3**	molecule 1	molecule 2
			Bond Lengths		
Pd−N(1)	2.011(4)	2.092(2)	2.008(3)	2.103(3)	2.113(3)
Pd−N(2)	2.044(4)	2.078(2)	2.039(3)	2.074(3)	2.072(3)
Pd−O(1)	1.985(3)		1.975(2)		
Pd−C(1)		1.973(2)		1.980(3)	1.983(3)
Pd−Cl	2.317(1)	2.3174(6)	2.3255(8)	2.3198(9)	2.3111(9)
			Bond Angles		
N(1)−Pd−N(2)	83.1(2)	82.95(7)	83.5(1)	81.7(1)	82.2(1)
N(1)−Pd−O(1)	175.1(1)		176.8(1)		
N(1)−Pd−C(1)		173.56(8)		172.5(1)	173.3(1)
N(1)−Pd−Cl	95.2(1)	94.37(5)	94.66(8)	93.82(9)	94.44(9)
N(2)−Pd−O(1)	94.1(1)		93.8(1)		
N(2)−Pd−C(1)		90.77(8)		91.9(1)	91.3(1)
N(2)−Pd−Cl	176.2(1)	176.64(5)	177.71(8)	175.41(8)	176.56(8)
O(1)−Pd−Cl	87.8(1)		88.12(7)		
C(1)−Pd−Cl		91.96(6)		92.6(1)	92.1(1)

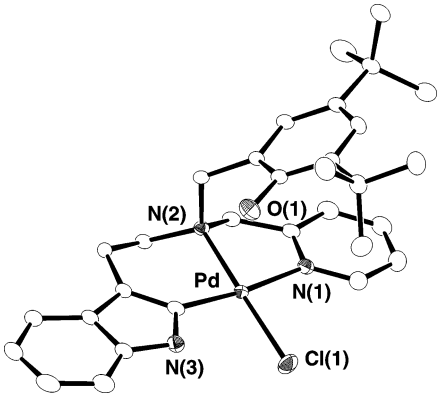

Figure 4. ORTEP view of [Pd(tbu-iepp-c)Cl] (**1b**) drawn with the thermal ellipsoids at the 50% probability level and the atomic labeling scheme.

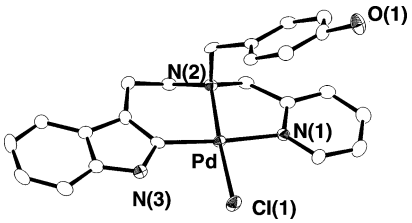

Figure 5. ORTEP view of [Pd(p-iepp-c)Cl] (**4**) drawn with the thermal ellipsoids at the 50% probability level and the atomic labeling scheme.

which may be ascribed to the difference in the trans effects of Pd−O and Pd−C bonds. The indole C2−C3 bond length in **1b** (1.379(3) Å) and **4** (1.375(5) and 1.374(6) Å) is only slightly longer than that of uncoordinated indole ring,[18,23,26] which is reminiscent of the corresponding bond length of an η^2-coordinated indole (1.379(7) Å).[18] The Pd(II)−C distance in **1b** and **4** is much shorter than that of the reported metal−indole complexes (Pd(II)−C3 = 2.12−2.15;[15] Cu(I)−C2 and Cu(I)−C3 = 2.23−2.27 Å[18]) but is within the normal range for other cyclopalladated complexes.[31−33] The phenol ring of **1b** and **4** is located above the coordinated pyridine ring to be involved in the intramolecular $\pi-\pi$ stacking. The shortest $C_{indole}-C_{pyridine}$ distance is 3.172(3) Å for **1b** and 3.060(5) and 3.133(5) Å for **4**, and the angle between the average planes of the two aromatic rings is 33.1° for **1b** and 37.5° and 58.4° for **4**. It is interesting to note in this connection that the side-chain phenol and indole rings stack only with the coordinated pyridine ring and do not stack with each other. This finding corresponds well with our previous observation on analogous complexes.[26]

Table 3. Absorption and Cyclic Voltammetric Data for Pd(II) Complexes in DMF

	wavelength/nm (ϵ/$M^{-1}cm^{-1}$)		*E*/*V* vs Ag/AgCl	
tbu-iepp (**1a**)	450 (940, sh)	340 (4100, sh)	0.97	1.08
tbu-iepp (**1b**)		290 (14000)	0.68	0.80
tbu-impp (**2**)	450 (920, sh)	340 (3900, sh)	0.89	1.01
tbu-miepp (**3**)	450 (900, sh)	340 (3900, sh)		
p-iepp (**4**)		295 (9200)	0.70	0.83

Characterization of the Complexes. (a) Spectral Properties. The absorption spectra of **1b** and **4** in DMF in the range 250−1000 nm exhibited a strong peak at 290 nm (ϵ = 14 000) and 295 nm (ϵ = 9200), respectively, while **1a**, **2**, and **3** showed peaks at 340 and 450 nm (Table 3), supporting that **2** has the same coordination structure as that of **1a** and **3**. Because the 450-nm peak is assigned to the phenolate-to-Pd(II) charge-transfer band (LMCT),[26] lack of this peak in **1b** and **4** indicates that the phenolate oxygen is not coordinated in these complexes in DMF, supporting that the Pd(II)−indole C2 bond is maintained in solution as well as in the solid state. The ^{1}H NMR chemical shifts for **1a** and **5** which is without a pendent aromatic ring are very similar, and this supports that the side-chain indole ring is not stacked with the coordinated pyridine ring in **1a**. On the other hand, large shift differences were observed between the indole protons of **1a** and **1b** in DMSO; the signals of indole C4, C5, and C7 protons in **1b** shifted downfield relative to those of **1a** with the chemical shift difference, $\Delta\delta = -(\delta - \delta_{\mathbf{1a}})$, of −0.1 to −0.6 ppm. These shifts which were also observed for **4** reflect σ-donation to Pd(II) by the indole ring and are in contrast with the rather small differences observed between the Cu(I)-η^2-coordinated indole and free indole.[18] A large upfield shift was detected for the indole NH proton ($\Delta\delta$ = 2.40 ppm).

(31) (a) Newkome, G. R.; Puckett, W. E.; Gupta, V. K.; Kiefer, G. E. *Chem. Rev*. **1986**, *86*, 451−489. (b) Yoneda, A.; Hakushi, T.; Newkome, G. R.; Morimoto, Y.; Yasuoka, N. *Chem. Lett*. **1994**, 175−176. (c) Orpen, A. G.; Brammer, L.; Allen, F. H.; Kennard, O.; Watson, D. G.; Taylor, R. *J. Chem. Soc., Dalton Trans*. **1989**, S1−S83. (d) Newkome, G. R.; Puckett, W. E.; Kiefer, G. E.; Gupta, V. K.; Fronczek, F. R.; Pantaleo, D. C.; McClure, G. L.; Simpson, J. B.; Deutsch, W. A. *Inorg. Chem*. **1985**, *24*, 811−826.
(32) Omae, I. *Organometallic Intramolecular-Coordination Compounds*; Elsevier Science Publishers: Amsterdam, NY, 1986.
(33) (a) Crabtree, R. H. *Chem. Rev*. **1985**, *85*, 245−269. (b) Alsters, P. L.; Engel, P. F.; Hogerheide, M. P.; Copijn, M.; Speck, A. L.; van Koten, G. *Organometallics* **1993**, *12*, 1831−1844.

Table 4. ^{1}H NMR Chemical Shifts (δ/ppm) and Upfield Shifts ($\Delta\delta$)[a] of Pyridine and Indole Proton Signals for Pd(II) Complexes in DMSO-d_6

	δ ($\Delta\delta$)/ppm				
	tbu-iepp (**1a**)	tbu-iepp (**1b**)	tbu-impp (**2**)	tbu-miepp (**3**)	tbu-pp (**5**)
py3	7.77	7.16 (+0.61)	7.01 (+0.76)	7.76 (+0.01)	7.63 (+0.14)
py4	8.11	7.65 (+0.46)	7.59 (+0.52)	8.07 (+0.04)	8.02 (+0.09)
py5	7.52	7.15 (+0.37)	6.91 (+0.61)	7.47 (+0.05)	7.48 (+0.04)
py6	8.69	8.44 (+0.25)	8.22 (+0.47)	8.65 (+0.04)	8.67 (+0.02)
in1	10.74	8.34 (+2.40)	10.97 (−0.23)		
in2	6.88		7.10 (−0.22)	6.86 (+0.02)	
in4	7.22	7.36 (−0.14)	8.04 (−0.82)	7.22 (0.0)	
in5	6.72	6.83 (−0.11)	6.91 (−0.19)	6.72 (0.0)	
in6	6.96	6.83 (+0.13)	7.10 (−0.14)	7.00 (−0.04)	
in7	6.72	7.29 (−0.57)	7.10 (−0.38)	6.66 (+0.06)	

[a] $\Delta\delta = -(\delta - \Delta\delta_{1a})$, where δ_{1a} refers to the shift for **1a**.

Complexes **1b** and **2** exhibited upfield shifts of the coordinated pyridine proton signals relative to those for **1a**, and the $\Delta\delta$ values (0.25−0.76 ppm) (Table 4) clearly show that the pyridine ring is stacked with the aromatic ring in solution. The NMR spectral behavior of **2** is very similar to that of the Pd(II) complexes of 2N1O-donor ligands with a pendent indole ring stacked with the pyridine ring.[26] These observations substantiate that the side-chain conformations as well as the coordination structures are maintained both in the solid state and in solution.

(b) Structural Changes. As expected from the conditions for isolation of **1a** and **1b**, conversion of **1a** to **1b** occurred in solution with the structural changes shown in Scheme 1. When the solution of **1a** in CH_3CN/CH_2Cl_2 was kept at room temperature for a few days, two kinds of crystals, orange crystals of **1a** and yellow crystals of **1b**, separated. The solution of **1b** in DMSO, on the other hand, exhibited a color change from yellow to orange with the appearance of a 450-nm peak of **1a** upon standing for 1 day at room temperature, indicating the conversion from **1b** to **1a**. This change was not observed in CH_3CN and CH_2Cl_2. Dependence of the interconversion on solvents may be due to the solubility of the complexes; **1b** is much less soluble in CH_3CN/CH_2Cl_2 than in DMSO and is not converted to **1a** in this solvent mixture, whereas conversion from **1a** to **1b** proceeds because **1b** crystallizes out of the solution. The ^{1}H NMR spectra indicated that the ratio of **1a** to **1b** was 1:0.3 in DMSO after 24 h at room temperature and 1:1 at 60 °C. Because of decomposition of **1b**, complete conversion of **1b** to **1a** was not possible at 100 °C and higher temperatures. To understand the mechanism of the conversion, we carried out an isotope-labeling experiment; deuterated **1b**, **1b-*d*$_{\text{phenol}}$** with the deuterated phenol moiety, was converted in DMSO-d_6 at 70 °C to **1a-*d*$_{\text{indole}}$** whose indole C2 position was over 85% deuterated, but nondeuterated **1b** did not give any indole-deuterated complex. The reaction of **1a** in 2:1 (v/v) CD_3CN/D_2O gave **1b** with the nondeuterated phenol moiety. No such conversion was detected for complex **4**, where coordination of the intramolecular phenolate oxygen is not possible. These results suggest that the phenol OH group takes part in the process of the structural conversion between **1a** and **1b**, where the chelate effect is inferred to be important and the phenolate oxygen abstracts the indole C2 proton to form **1b**. Complex **1b** separated from the solution as soon as it was formed, and this may explain why the phenol OH group was not deuterated in the above experiment. It is generally agreed that cyclopalladation reactions of aryl compounds proceed by an electrophilic substitution mechanism.[34] The rate-determining step in such processes is the C−H bond cleavage, which is normally regarded as an irreversible process.[34,36] In reversible cyclopalladation reactions of aromatic ligands, on the other hand, kinetically controlled isomers have been reported to be different from thermodynamically controlled isomers,[35] which explains the present structural conversion where the phenolate complex **1a** is kinetically favored and the cyclopalladated complex **1b** is thermodynamically favored in CH_3CN. Our results indicate that the C−H bond scission is a reversible step in the present interconversion between **1a** and **1b**. The energy gap between **1a** and **1b**, ΔE, was estimated from the van't Hoff plot using the ^{1}H NMR data in DMSO (see Experimental Section) to be 15 kJ mol^{-1}, which is relatively large when compared with the rather small enthalpy of formation (60−120 kJ mol^{-1}) of a Pd−C bond by cyclopalladation.[34,36]

Formation of the Pd(II)−indole σ-bond observed for **1b** and **4** may be related with the favorable six-membered chelate ring formed by the indole C2 and amine nitrogen atoms. We infer from the structures of **1b** and **2** that the observed structural difference is a consequence of the steric requirements for the side-chain indole ring to approach the Pd center.[18] Considering that complex **3** containing an *N*-methylindole moiety instead of the NH−indole in **1a** did not undergo the conversion to Pd−indole species under a similar condition of **1b** formation, the conversion may require dissociation of the indole−NH proton, which is considered to be analogous to the tautomeric proton migration giving the 3*H*-indole ring in some Pd complexes with Pd(II)−C3 and −N1 bindings.[14,15,17]

Redox Properties. Oxidation of **1b** by 1 equiv of Ce(IV) in DMF at −60 °C caused a color change from yellow to green, giving a new peak at 550 nm in the visible absorption spectrum (Figure 6). The reaction was found to be a one-electron oxidation process from the reaction stoichiometry. Complex **4** was also oxidized to exhibit a similar absorption peak at 551 nm. The ESR spectra of oxidized **1b** and **4** exhibited a new sharp signal at $g = 2.004$, and the amount of unpaired electron was calculated to be more than 0.90 from the integrated spectrum. On the other hand, the absorption spectra of **1a** and **3** remained unchanged upon addition of Ce(IV), and no peaks characteristic of the phenoxyl radical[25,37,38] were observed. The oxidized species of

(34) (a) Parshall, G. W *Acc. Chem. Res*. **1970**, *3*, 139−144. (b) Ryabov, A. D. *Chem. Rev*. **1990**, *90*, 403−424. (c) Beller, M.; Riermeier, T. H.; Haber, S.; Kleiner, H.-J.; Herrmann, W. A. *Chem. Ber*. **1996**, *129*, 1259−1264.
(35) (a) O'Keefe, B. J.; Steel, P. J. *Inorg. Chem. Commun*. **1999**, *2*, 10−13. (b) O'Keefe, B. J.; Steel, P. J. *Organometallics* **2003**, *22*, 1281−1292.
(36) Gómez, M.; Granell, J.; Martinez, M. *Eur. J. Inorg. Chem*. **2000**, 217−224.
(37) (a) Halfen, J. A.; Young, V. G., Jr.; Tolman, W. B. *Angew. Chem., Int. Ed. Engl*. **1996**, *35*, 1687−1690. (b) Halfen, J. A.; Jazdzewski, B. A.; Mahapatra, S.; Berreau, L. M.; Wilkinson, E. C.; Que, L., Jr.; Tolman, W. B. *J. Am. Chem. Soc*. **1997**, *119*, 8217−8227. (c) Sokolowski, A.; Leutbecher, H.; Weyhermüller, T.; Schnepf, R.; Bothe, E.; Bill, E.; Hildebrandt, P.; Wieghardt, K. *J. Biol. Inorg. Chem*. **1997**, *2*, 444−453. (d) Zurita, D.; Gautier-Luneau, I.; Ménage, S.; Pierre, J.-L.; Saint-Aman, E. *J. Biol. Inorg. Chem*. **1997**, *2*, 46−55. (e) Jazdzewski, B. A.; Young, V. G., Jr.; Tolman, W. B. *Chem. Commun*. **1998**, 2521−2522. (f) Benisvy, L.; Blake, A. J.; Collison, D.; Davis, E. S.; Garner, C. D.; McInnes, E. J. L.; McMaster, J.; Whittaker, G.; Wilson, C. *Chem. Commun*. **2001**, 1824−1826. (g) Thomas, F.; Gellon, G.; Gautier-Luneau, I.; Saint-Aman, E.; Pierre, J.-L. *Angew. Chem., Int. Ed*. **2002**, *41*, 3047−3050. (h) Shimazaki, Y.; Huth, S.; Hirota, S.; Yamauchi, O. *Inorg. Chim. Acta* **2002**, *331*, 168−177.
(38) (a) Sokolowski, A.; Müller, J.; Weyhermüller, T.; Schnepf, R.; Hildebrandt, P.; Hildebrandt, K.; Bothe, E.; Wieghardt, K. *J. Am. Chem. Soc*. **1997**, *119*, 8889−8900. (b) Sokolowski, A.; Adam, B.; Weyhermüller, T.; Kikuchi, A.; Hildebrandt, K.; Schnepf, R.; Hildebrandt, P.; Bill, E.; Wieghardt, K. *Inorg. Chem*. **1997**, *36*, 3702−3710. (c) Shimazaki, Y.; Tani, F.; Fukui, K.; Naruta, Y.; Yamauchi, O. *J. Am. Chem. Soc*. **2003**, *125*, 10512−10513.

Scheme 1. Interconversion between [Pd(tbu-iepp)Cl] Isomers **1a** and **1b** and Indole Ring Deuteration (*tert*-Butyl Groups Are Omitted for Clarity in the Complexes)

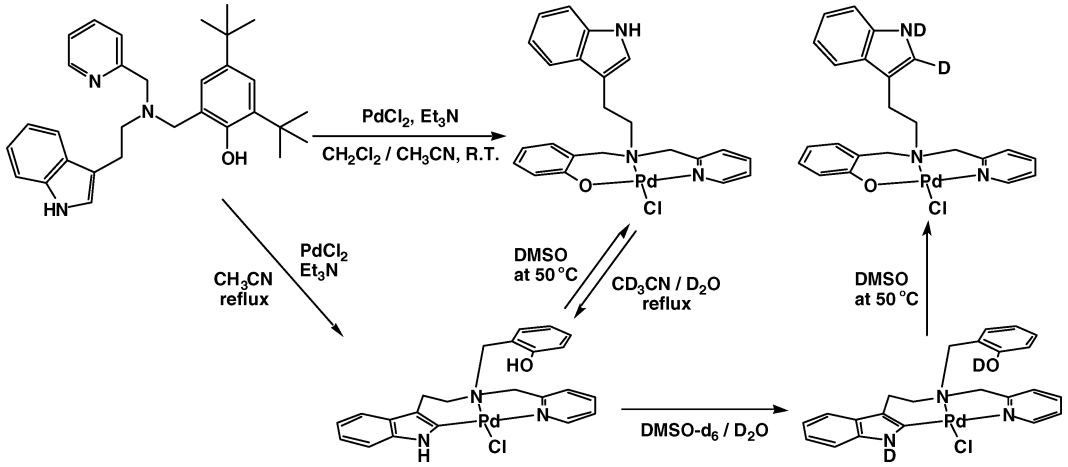

1b and **4** are considered to assume one of the three possible forms, an indole radical, a phenoxyl radical, or a Pd(III) complex. Mononuclear Pd(III) complexes are relatively uncommon; the two well-characterized examples are $[Pd([9]\text{-}aneS_3)_2]^{3+}$ ([9]-$aneS_3$ = 1,4,7-trithiacyclononane)[39] and $[Pd([9]\text{-}aneN_3)_2]^{3+}$ ([9]-$aneN_3$ = 1,4,7-triazacyclononane),[40] both of which have been structurally characterized by X-ray analysis. Several others have been generated electrochemically or otherwise studied in situ.[41,42] It has been reported that a Pd(III) complex, $[Pd([9]\text{-}aneN_3)_2]^{3+}$, exhibits the absorption peaks at 383 nm (ϵ = 590 M^{-1} cm^{-1}) and 314 nm (ϵ = 1240 M^{-1} cm^{-1}) and that $[Pd([9]\text{-}aneS_3)_2]^{3+}$ exhibits a peak at 475 nm (ϵ = 3000 M^{-1} cm^{-1}).[39,40] The ESR spectra of these Pd(III) complexes showed a broad isotropic or anisotropic signal based on the $^2A_{1g}$ ground spin state in the range g = 2.005−2.123.[39−41] The spectral properties of oxidized **1b** and **4** are very different from those of the Pd(III) complexes, and the sharp signal at g = 2.004 exhibited by **1b** and **4** indicates the formation of an organic radical species of the Pd(II) complexes (Figure 7), although the g value is slightly larger than the value of 2.001 expected for organic radicals and no nitrogen superhyperfine structures were observed. While the di(*tert*-butyl)phenoxyl radical species has been reported to show a characteristic intense absorption band at about 400 nm due to the $\pi-\pi^*$ transition of the phenoxyl radical,[25,37,38] oxidized **1b** and **4** did not show this band. When the green solution of oxidized **1b** in DMF was left to stand at −60 °C, it rapidly turned yellow, and the 550-nm absorption peak disappeared in the first-order decay (Figure 6). The half-life, $t_{1/2}$, of oxidized **1b** and **4** was calculated to be 20 (k_{obs} = 3.5×10^{-2} s^{-1}) and 18 s (k_{obs} = 3.9×10^{-2} s^{-1}), respectively. This shows that despite the difference in the phenol ring substituents oxidized **1b** and **4** exhibit similar stability, which is in contrast with the dependence of the stability of the phenoxyl radical−metal complexes on phenol ring substituents.[25] These results exclude the possibility that the radical is assigned to the phenoxyl radical. On the other hand, the indole radicals from tryptophan and *N*-methylindole have been reported to show a characteristic absorption band in the region 510−560 nm,[4,22] where the indole-π-cation radical and the neutral indolyl radical give a band centered at 560 and 510 nm, respectively. On the basis of these considerations, we assign the oxidized forms of **1b** and **4** having a peak at ∼550 nm to the indole π-cation radical species, whose unpaired electron is inferred to be

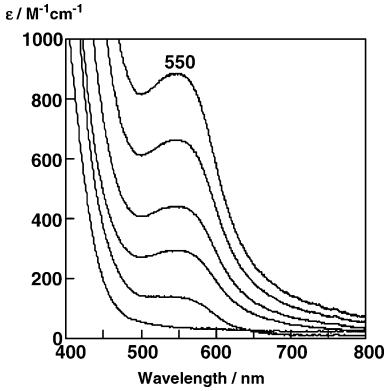

Figure 6. Absorption spectral changes of oxidized **1b** with time in DMF at −60 °C (5.0×10^{-4} M). The spectra were recorded at 10-s intervals.

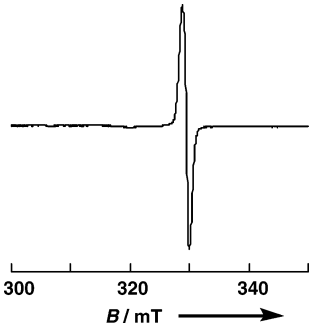

Figure 7. ESR spectrum of one-electron-oxidized **1b** in DMF at 77 K. Concentration: 5.0×10^{-4} M; microwave power, 1 mW; modulation amplitude, 0.63 mT.

(39) (a) Blake, A. J.; Holder, A. J.; Hyde, T. I.; Schröder, M. *J. Chem. Soc., Chem. Commun.* **1987**, 987−988. (b) Blake, A. J.; Holder, A. J.; Hyde, T. I.; Roverts, Y. V.; Lavery, A. J.; Schröder, M. *J. Organomet. Chem.* **1987**, *323*, 261−270.

(40) (a) Blake, A. J.; Gordon, L. M.; Holder, A. J.; Hyde, T. I.; Reid, G.; Schröder, M. *J. Chem. Soc., Chem. Commun.* **1988**, 1452−1454. (b) McAuley, A.; Whitcombe, T. W. *Inorg. Chem.* **1988**, *27*, 3090−3099.

(41) (a) Kirmse, R.; Stach, J.; Dietzsch, W.; Steimecke, G.; Hoyer, E. *Inorg. Chem.* **1980**, *19*, 2679−2685. (b) Chandrasekhar, S.; McAuley, A. *Inorg. Chem.* **1992**, *31*, 2663−2665. (c) Möller, E.; Kirmse, R. *Inorg. Chim. Acta* **1997**, *257*, 273−274. (d) Jasper, S. A., Jr.; Huffman, J. C.; Todd, L. J. *Inorg. Chem.* **1998**, *37*, 6060−6064. (e) Blake, A. J.; Raid, G.; Schröder, M. *J. Chem. Soc., Dalton Trans.* **1990**, 3363−3373. (f) Raid, G.; Blake, A. J.; Hyde, T. I.; Schröder, M. *J. Chem. Soc., Chem. Commun.* **1988**, 1397−1399.

(42) (a) Warren, L. F., Jr.; Hawthorne, M. F. *J. Am. Chem. Soc.* **1968**, *90*, 4823−4828. (b) Warren, L. F., Jr.; Hawthorne, M. F. *J. Am. Chem. Soc.* **1970**, *92*, 1157−1173. (c) Grant, G. J.; Sanders, K. A.; Setzer, W. N.; VanDerveer, D. G. *Inorg. Chem.* **1991**, *30*, 4053−4056.

localized in the indole ring. The relatively short half-life of these radical species indicates that they are less stable than the metal−phenoxyl and other metal−organic radical species.[25,37,38]

Table 3 shows the redox potentials of **1a**, **1b**, **2**, and **4** measured in DMF under anaerobic conditions at a scan rate of 100 mV/s in the range 0−1.5 V where no Pd redox wave was observed. Complexes **1a**, **1b**, and **4** exhibited two irreversible oxidation peaks (**1a**, 0.97 and 1.08 V; **1b**, 0.68 and 0.80 V; **4**, 0.70 and 0.83 V (vs Ag/AgCl)). Considering that the redox potential of a Cu(II)-coordinated phenolate oxygen is lower than that of free phenol and that the potential of the indole ring is higher than that of the phenol ring,[4,22] the first oxidation peak of **1a** is assigned to the oxidation of the coordinated phenolate moiety and the second one is assigned to that of the indole ring. On the other hand, the first and second oxidation peaks of **1b** and **4** are assigned to the oxidation of the coordinated indole and free phenol rings, respectively, because the oxidation potential of the second peak agrees well with that of the phenol moiety weakly coordinated to Cu(II).[37] The redox potential of the indole ring of **1b** and **4** was found to be lower than that of **1a**, which shows that the Pd(II)-bound indole moiety is more easily oxidized than the unbound one.

Conclusion

We prepared and characterized the Pd(II) complexes of a series of new tripod-like 2N1O-donor ligands with a phenol ring and a pendent indole moiety. The direct indole carbon−Pd(II) bonding has been established by the molecular structure of **1b** and **4**, which was also concluded for the solution of **1b** in DMSO-d_6 by the downfield shifts of the indole protons due to effective σ-donation by the C2 atom. Complexes **1a** and **1b** were interconvertible in CH_3CN and DMSO as shown in Scheme 1. One-electron chemical and electrochemical oxidations of the Pd(II)−indole complexes, **1b** and **4**, yielded the corresponding Pd(II)−indole π-cation radical species, which is supported by the characteristic 550-nm absorption peak and the ESR signal of the radical species. To the best of our knowledge, this is the first observation of the indole π-cation radical species in metal complexes.

The heme site of C*c*P has two tryptophyl residues, and one of them, Trp 191, is known to give an indolyl radical species in the course of the reaction.[4,8,20] The active-site structure of the enzyme[43] shows that both coordinated histidine (His 175) and Trp 191 are hydrogen-bonded to a proximal aspartyl residue (Asp 235), which should affect the electron density of the indole ring.[8] Pd(II)−indole C2 bonding with deprotonation facilitates the indole radical formation as seen from the lower redox potential (Table 3) and may be compared with the Cu(II)−phenolate oxygen bonding in galactose oxidase. There has been no information of direct metal−indole interactions in biological systems, but our results suggest that the indole NH−Asp 235 hydrogen bond may make the indole ring negatively charged and thus favor the radical formation.

The present findings demonstrate the versatile nature of the indole ring in the Pd(II) coordination sphere and will provide further information on its functions in chemical and biological systems.

Acknowledgment. We gratefully acknowledge the support of this work by a Grant-in-Aid for Scientific Research (No. 13440202 to O.Y.) from the Ministry of Education, Culture, Sports, Science, and Technology of Japan. This work was supported in part by the Kansai University Grant-in-Aid for Faculty Joint Research Program, 2002, and the "Nanotechnology Support Project" of the Ministry of Education, Culture, Sports, Science, and Technology of Japan, for which we express our sincere thanks.

Supporting Information Available: X-ray crystallographic data (CIF) for complexes **1a**, **1b**, **3**, and **4**, and ^{1}H NMR spectra showing the interconversion. This material is available free of charge via the Internet at http://pubs.acs.org.

JA031587V

(43) Finzel, B. C.; Poulos, T. L.; Kraut, J. *J. Biol. Chem.* **1984**, *259*, 13027−13036.